




Iron(III), nickel(II) and zinc(II) complexes based on acetophenone-S-methyl-thiosemicarbazone: synthesis, characterization, thermogravimetry, and a structural study

Yasemin Kurt & Nahide Gulsah Deniz


To cite this article: Yasemin Kurt & Nahide Gulsah Deniz (2015) Iron(III), nickel(II) and zinc(II) complexes based on acetophenone-S-methyl-thiosemicarbazone: synthesis, characterization, thermogravimetry, and a structural study, Journal of Coordination Chemistry, 68:22, 4070-4081, DOI: [10.1080/00958972.2015.1086760](https://doi.org/10.1080/00958972.2015.1086760)

To link to this article: <http://dx.doi.org/10.1080/00958972.2015.1086760>

 View supplementary material 

 Accepted author version posted online: 26 Aug 2015.
Published online: 14 Sep 2015.

 Submit your article to this journal 

 Article views: 136

 View related articles 

 View Crossmark data 

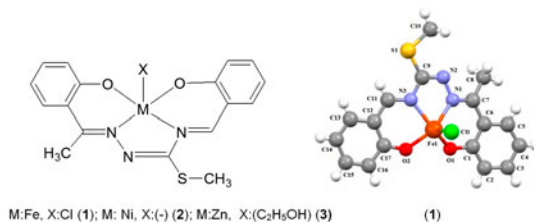
Iron(III), nickel(II) and zinc(II) complexes based on acetophenone-*S*-methyl-thiosemicarbazone: synthesis, characterization, thermogravimetry, and a structural study

YASEMIN KURT*[†] and NAHIDE GULSAH DENIZ[‡]

[†]Division of Inorganic Chemistry, Department of Chemistry, Istanbul University, Istanbul, Turkey

[‡]Division of Organic Chemistry, Department of Chemistry, Istanbul University, Istanbul, Turkey

(Received 1 February 2015; accepted 6 August 2015)



New complexes, [Fe(L)Cl], [Ni(L)], and [Zn(L)C₂H₅OH] (**1–3**), were synthesized by template reaction of 2-hydroxyacetophenone-*S*-methyl-thiosemicarbazone with 2-hydroxy-benzaldehyde. The compounds were characterized by elemental analysis, magnetic measurements, FT-IR, ¹H NMR, UV–visible, and ESI–MS spectra. In these complexes, the ligand is coordinated to the metal ion as dinegatively charged tetradentate chelating agents via the N₂O₂ donor set. The iron(III) and zinc(II) complexes exhibit square pyramidal geometry whereas the nickel(II) complex has a square planar geometry. The crystal structure of **1**, determined by X-ray diffraction method, indicates that **1** crystallizes in the monoclinic space group *P21/c* with *Z* = 4. Thermal decompositions of the compounds have been investigated using TGA in air.

Keywords: Thiosemicarbazone; Acetophenone; N₂O₂ complex; Crystal structure; Thermogravimetric analysis

1. Introduction

The chemistry of thiosemicarbazones has attracted interest primarily due to their biological activities such as antituberculous [1], antitumor [2], antimicrobial [3], antiviral [4], antioxidant [5], and cytotoxic [6] effects. The biological activity of such compounds is related to their chelating ability with transition metal ions, a consequence of the unique characteristics of mixed hard–soft *NS* donors [7].

Thiosemicarbazones have various coordination modes due to their geometrical flexibility and polydentate nature. Common metal complexes of thiosemicarbazones have bidentate

*Corresponding author. Email: dasdemir@istanbul.edu.tr

and tridentate functions through the sulfur, azomethine nitrogen, and hetero atom of an arylidene moiety [8]. Some tetradentate thiosemicarbazones are synthesized by template condensation in the presence of transition metal ions. Many template compounds synthesized from *S*-alkyl-thiosemicarbazones with iron(III), nickel(II) [9–14], zinc(II) [15, 16], copper(II), cobalt(II) [1, 17, 18], vanadyl(IV) [19], and uranyl(VI) [20] ions have been investigated.

The N_2O_2 -type metal complexes of bis(arylidene)-*S*-alkyl-thiosemicarbazones are usually obtained from substituted 2-hydroxy benzaldehydes, but there are a limited number of such complexes that include an acetophenone moiety. A few N_2O_2 complexes obtained by template reaction of acetophenone thiosemicarbazones and 2-hydroxy benzaldehyde with copper(II), nickel(II), vanadyl(IV), and uranyl(VI) ions have been reported [21–23].

In this study, iron(III), nickel(II), and zinc(II) complexes (**1–3**) of tetradentate N^1, N^4 -diarylidene-*S*-methyl-thiosemicarbazone ligands were synthesized using 2-hydroxyacetophenone-*S*-methyl-thiosemicarbazone and salicylaldehyde as starting compounds (figure 1). The new complexes and the starting thiosemicarbazone were characterized by elemental analysis, magnetic measurements, FT-IR, 1H NMR, UV–visible, ESI–MS spectra, and thermogravimetric analysis (TGA). The crystal structure of chlorido N^1 -[(2-hydroxyphenyl) ethylidene]- N^4 -[(2-hydroxyphenyl)methylidene]-*S*-methyl-thiosemicarbazidato-iron (III) (**1**) was determined by X-ray diffraction.

2. Experimental

2.1. Materials and physical measurements

All chemicals were reagent grade and used as commercially purchased without purification. Elemental analyses were determined on a Thermo Finnigan Flash EA 1112

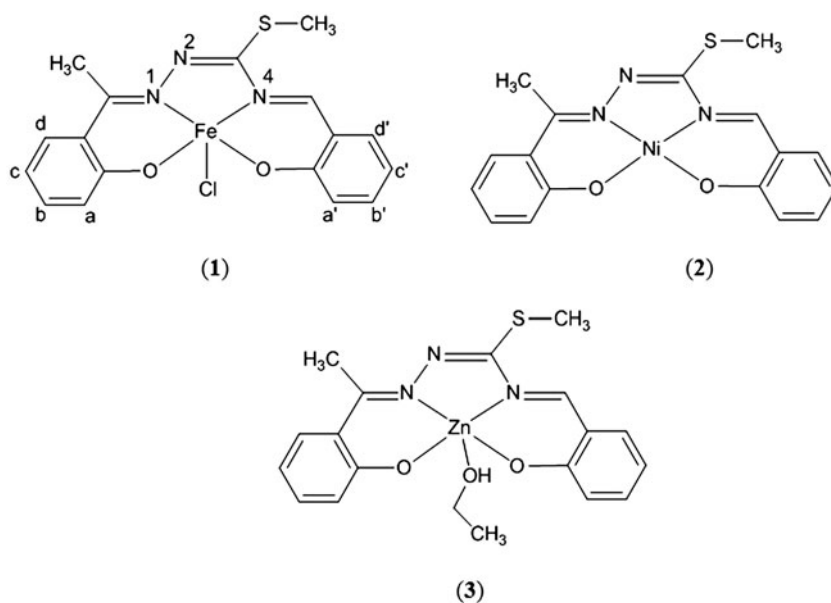


Figure 1. [Fe(L)Cl] (**1**), [Ni(L)] (**2**), and [Zn(L)C₂H₅OH] (**3**).

Series elemental analyzer. Magnetic measurements were carried out at room temperature with a Sherwood Scientific MK I apparatus using $\text{CuSO}_4 \cdot 5\text{H}_2\text{O}$ as calibrant. IR spectra were measured on an Agilent Technologies Cary 630 FT-IR-spectrophotometer by means of attenuated total reflection (ATR) techniques. ^1H NMR spectra were recorded on a Bruker Avance-500 model spectrometer relative to SiMe_4 using DMSO-d_6 . Electronic spectra of the compounds were recorded in 2×10^{-5} M DMF solution with a Shimadzu UV-2600 UV-vis spectrophotometer from 200 to 900 nm. The ESI-MS analyses were carried out in positive ion mode using a Thermo Finnigan LCQ Advantage MAX LC/MS/MS. Thermal degradation experiments were carried out on a Shimadzu TGA-50 thermogravimetric analyzer. A constant heating rate of 10 K min^{-1} was used between room temperature and 900°C . The air flow rate was 50 mL min^{-1} for thermo-oxidative degradation runs. Sample weights were 16–18 mg in all cases.

2.2. Synthesis of the starting ligand

2-Hydroxy-acetophenone-*S*-methyl-thiosemicarbazone was prepared with small modifications of the literature method [24].

H_2L^1 . Light yellow, m.p. $100.6\text{--}101.0^\circ\text{C}$, 70%. Anal. Calcd for $\text{C}_{10}\text{H}_{13}\text{N}_3\text{OS}$ ($223.29 \text{ g mol}^{-1}$) (%): C, 53.79; H, 5.87; N, 18.82; S, 14.36. Found: C, 53.58; H, 5.69; N, 19.01; S, 13.99. ATR (selected bands, cm^{-1}): $\nu(\text{NH})_{\text{asy}}$ 3420, $\nu(\text{NH})_{\text{sy}}$ 3309, $\nu(2\text{-OH})$ 3161, $\delta(\text{N}^4\text{H})$ 1646, $\nu(\text{C}=\text{N}^1)$ 1600, $\nu(\text{N}^2=\text{C})$ 1592, $\nu(\text{C}-\text{O})$ 1130, $\nu(\text{C}-\text{S})$ 749. ^1H NMR (500 MHz, DMSO-d_6 , ppm): 13.33, 13.10 (*cis/trans* ratio: 2/1, s, 1H, 2-OH), 7.54 (ddd, $J = 16.11, 7.81, 1.46$, 1H, d), 7.20 (ddd, $J = 14.64, 7.32, 1.46$, 1H, b), 6.85 (ddd, $J = 14.15, 7.32, 1.46$, 1H, c), 6.81 (dd, $J = 8.29, 1.46$, 1H, a), 6.67 (s, 2H, NH_2), 2.43 (s, 3H, S- CH_3), 2.40 (s, 3H, C- CH_3). UV-vis [λ_{max} ($\log \epsilon$), nm ($\text{dm}^3 \text{ cm}^{-1} \text{ mol}^{-1}$): 260 (4.29), 293 (4.47), 302 sh. (4.45), 335 (3.52). ESI-MS (positive ion mode), m/z : obsv. 224.52, Calcd 224.08 ($[\text{M} + \text{H}]^+$, 100%); obsv. 115.11, Calcd 115.02 ($[\text{M}-\text{C}_6\text{H}_4\text{OH}-\text{CH}_3]^+$, 12.48%); obsv. 68.48, Calcd 68.02 ($[\text{M}-\text{C}_6\text{H}_4\text{OH}-\text{SCH}_3-\text{CH}_3]^+$, 5.04%).

2.3. Synthesis of the complexes

$[\text{Fe}(\text{L})\text{Cl}]$ (**1**). Complex **1** was prepared with the procedure given in a previous article [11]. 2-Hydroxy-acetophenone-*S*-methyl-thiosemicarbazone (0.223 g, 1 mmol) and 2-hydroxybenzaldehyde (0.146 g, 1 mmol) were added dropwise to solution of $\text{FeCl}_3 \cdot 6\text{H}_2\text{O}$ (0.27 g, 1 mmol) in 10 mL absolute ethyl alcohol. After a week, black precipitate was filtered off, washed with a small portion of cold ethanol and diethyl ether, and dried in vacuo.

The nickel(II) and zinc(II) complexes (**2** and **3**) were synthesized in a similar manner using $\text{Zn}(\text{CH}_3\text{COO})_2 \cdot 2\text{H}_2\text{O}$ and $\text{Cu}(\text{CH}_3\text{COO})_2 \cdot 2\text{H}_2\text{O}$ salts. The analytical and spectroscopic data of **1–3** follow:

$[\text{Fe}(\text{L})\text{Cl}]$ (**1**). Black, m.p. $> 350^\circ\text{C}$, yield 19%, μ_{eff} : 5.89 BM. Anal. Calcd for $\text{C}_{17}\text{H}_{15}\text{N}_3\text{O}_2\text{SClFe}$ ($416.68 \text{ g mol}^{-1}$) (%): C, 49.00; H, 3.63; N, 10.08; S, 7.70. Found: C, 48.88; H, 3.52; N, 9.88; S 7.60. ATR (selected bands, cm^{-1}): $\nu(\text{C}=\text{N})$ 1607, 1569 br, $\nu(\text{C}-\text{O})_{\text{arom}}$ 1153, 1130, $\nu(\text{C}-\text{S})$ 761. UV-vis [λ_{max} ($\log \epsilon$), nm ($\text{dm}^3 \text{ cm}^{-1} \text{ mol}^{-1}$): 265 (4.45), 278 (4.40), 300 (4.40), 392 (4.08), 462 (3.89). ESI-MS (positive ion mode), m/z : obsv. 381.02, Calcd 381.10 ($[\text{FeLCl}-\text{Cl}]^+$, 100%); obsv. 438.90, Calcd 438.98 ($[\text{FeLCl} + \text{Na}]^+$, 6.53%).

$[Ni(L)]$ (2). Claret red, m.p. 314.0–315.6 °C, yield 39%, μ_{eff} : 0.26 BM. Anal. Calcd for $C_{17}H_{15}N_3O_2SNi$ (384.07 g mol⁻¹) (%): C, 53.16; H, 3.94; N, 10.94; S, 8.35%. Found: C, 53.14; H, 3.91; N, 11.00; S, 8.25. ATR (selected bands, cm⁻¹): $\nu(C=N)$ 1615, 1607, 1576, $\nu(C-O)_{\text{arom}}$ 1169, 1146 $\nu(C-S)$ 746. ¹H NMR (500 MHz, DMSO-d₆, ppm): 8.28 (s, 1H, N⁴=CH), 7.75 (d, J = 8.3, 2H, d,d'), 7.45 (tt, J = 6.83, 1.96, 1H, b'), 7.26 (tt, J = 6.83, 1.46, 1H, b), 6.97 (d, J = 8.79, 1.46, 1H, a'), 6.69 (dt, J = 18.54, 6.83, 2H, c,c'), 2.86 (s, 3H, S-CH₃), 2.74 (s, 3H, -C-CH₃). UV-vis [λ_{max} (log ϵ), nm (dm³ cm⁻¹ mol⁻¹): 264 (4.70), 302 (4.49), 323 (4.35), 405 (4.42), 487 (4.02), 560 (3.81). ESI-MS (positive ion mode), m/z : obsv. 384.20, Calcd 384.03 ([NiL + H]⁺, 100%); obsv. 406.12, Calcd 406.01 ([NiL + Na]⁺, 22.47%).

$[Zn(L)C_2H_5OH]$ (3). Orange, m.p. > 350 °C, yield 73%, μ_{eff} : diamag. Anal. Calcd for $C_{17}H_{15}N_3O_2SZn \cdot C_2H_5OH$ (436.86 g mol⁻¹) (%): C, 53.16; H, 3.94; N, 10.94; S, 8.35%. Found: C, 53.05; H, 4.08; N, 7.72; S, 5.89. ATR (selected bands, cm⁻¹): $\nu(C=N)$ 1610, 1598, 1574, $\nu(C-O)_{\text{arom}}$ 1161, 1142, $\nu(C-S)$ 746. ¹H NMR (500 MHz, DMSO-d₆, ppm): 8.61 (s, 1H, N⁴ = CH), 7.59 (dd, J = 8.29, 1.95 1H, d), 7.46 (dd, J = 8.30, 1.95, 1H, d'), 7.37 (ddd, J = 8.79, 6.83, 1.95, 1H, b'), 7.16 (ddd, J = 8.30, 6.83, 1.47, 1H, b), 6.72 (d, J = 8.79, 1H, a'), 6.71 (d, J = 8.29, 1H, a), 6.54 (td, J = 7.81, 0.97, 1H, c'), 6.50 (td, J = 8.29, 1.46, 1H, c), 4.61 (t, J = 5.36, ethyl alcohol -OH), 3.61–3.63 (m, 2H, ethyl alcohol -CH₂), 2.72 (s, 3H, S-CH₃), 2.62 (s, 3H, -C-CH₃), 1.24 (t, J = 6.34, H, ethyl alcohol -CH₃). UV-vis [λ_{max} (log ϵ), nm (dm³ cm⁻¹ mol⁻¹): 264 (4.46), 307 (4.56), 332 (4.45), 430 (4.33), 473 (4.29). ESI-MS (positive ion mode) m/z : obsv. 390.20, Calcd 390.02 ([ZnL + H]⁺, 100%); obsv. 343.20, Calcd 343.02 ([ZnL-SCH₃ + H]⁺, 5.06%); obsv. 328.30, Calcd 328.00 ([ZnL-SCH₃-CH₃ + H]⁺, 4.25%).

2.4. Crystal structure determination and refinement

Single black crystals of **1** for X-ray diffraction analysis were obtained by slow evaporation of ethanol solution at room temperature. In **1**, $C_{17}H_{15}N_3O_2S_1Cl_1Fe_1$, having approximate dimension of 0.55 × 0.40 × 0.10 mm was mounted on a glass fiber. The data were collected at room temperature to maximum θ values of 30.5° for **1**. All measurements were made on a Rigaku R-Axis Rapid-S imaging plate area detector with monochromated Mo K α radiation (λ = 0.71070 Å). Experimental conditions are summarized in table 1. The crystal structure was solved by SIR 92 [25] and refined with CRYSTALS software package [26]. The non-hydrogen atoms were refined anisotropically. Hydrogens were located in geometrically idealized positions (C–H = 0.95(6) Å) and treated as riding with $U_{\text{iso}}(\text{H}) = 1.2U_{\text{eq}}(\text{C})$. The selected bond distances, bond and torsion angles for **1** are listed in tables 2–4, respectively. The conformational angles for **1** are given in table 5. Molecular drawing was performed with the program ORTEP-III [27] with 50% probability displacement ellipsoids for **1** in figure 2. The intermolecular hydrogen bond parameters of **1** are illustrated in figure 3.

3. Results and discussion

3.1. Synthesis and physical properties

2-Hydroxy-acetophenone-*S*-methyl-thiosemicarbazone in form of powder crystals is soluble in common solvents. Reactions of the thiosemicarbazone with 2-hydroxy-benzaldehyde in

Table 1. Crystal data and structure refinement for **1**.

Empirical formula	C ₁₇ H ₁₅ N ₃ O ₂ S ₁ Cl ₁ Fe ₁
Crystal color, habit	Black, chunk
Crystal size (mm)	0.55 × 0.40 × 0.10
Formula weight	416.69
Temperature (K)	293.5(2)
Wavelength (Å)	0.71073
Crystal system	Monoclinic
Space group	<i>P</i> 2 ₁ / <i>c</i>
Cell dimensions	<i>a</i> = 11.6337(5) Å <i>b</i> = 8.5945(3) Å <i>c</i> = 18.0493(9) Å β = 103.708(3) ^o
Cell volume (Å ³)	1753.27(13)
Cell formula units (<i>Z</i>)	4
<i>D</i> _{calcd} (g cm ⁻³)	1.579
Absorption coefficient (mm ⁻¹)	1.147
<i>F</i> (0 0 0)	852.00
<i>h, k, l</i> ranges	-16/16, -12/11, -25/25
Reflections collected	12,754
Independent reflections	5257 [<i>R</i> _{int} = 0.069]
Data/restraints/parameters	4881/0/342
Goodness-of-fit (GOF) on <i>F</i>	1.181
Final <i>R</i> indices [<i>I</i> > 2σ(<i>I</i>)]	<i>R</i> = 0.046, <i>wR</i> = 0.083
Largest diff. peak and hole (e Å ⁻³)	0.042 and -0.042

Table 2. The iron(III)-centered bond distances of **1** (Å).

Fe1–O1	1.864(3)	Fe1–N3	2.076(3)
Fe1–O2	1.910(2)	Fe1–Cl1	2.221(1)
Fe1–N1	2.096(3)		

Table 3. The Fe(III)-centered angles of **1** (°).

Cl1–Fe1–O1	110.66(9)	O1–Fe1–N1	85.7(1)
Cl1–Fe1–O2	107.01(8)	N3–Fe1–N1	75.1(1)
Cl1–Fe1–N1	101.51(8)	C17–O2–Fe1	132.0(2)
Cl1–Fe1–N3	104.00(9)	C1–O1–Fe1	129.1(2)
O2–Fe1–O1	94.6(1)	C9–N3–Fe1	113.4(2)
O2–Fe1–N3	86.9(1)	C11–N3–Fe1	127.2(2)
O2–Fe1–N1	149.3(1)	C7–N1–Fe1	129.2(2)
O1–Fe1–N3	143.1(1)	Fe1–N1–N2	115.0(2)

the presence of iron(III), nickel(II), and zinc(II) in ethyl alcohol yielded stable complexes as shown in figure 1. The N₂O₂ complexes (**1–3**) form as very fine crystal materials, soluble in common organic solvents. Complex **1** is stable in air and the magnetic susceptibility values are compatible with high-spin d⁵ iron(III) center. The low magnetic susceptibility values of **2** indicate square planar environment of nickel(II) center in the N₂O₂ chelate.

3.2. Spectroscopic data

3.2.1. ¹H NMR spectra. In ¹H NMR spectra of H₂L¹ and template complexes (**2** and **3**), the expected chemical shift values are monitored for aromatic, azomethine, and *S*-methyl protons [28]. The 2-OH proton of ligand is observed at 13.33 and 13.10 ppm as two

Table 4. Selected torsion angles of **1** (°).

C11–Fe1–O2–C17	84.0(3)	N3–Fe1–N1–C7	–169.1(3)
C11–Fe1–O1–C1	–65.7(3)	C10–S1–C9–N2	1.8(3)
O1–Fe1–O2–C17	–162.8(3)	N1–N2–C9–N3	–0.8(4)
N3–Fe1–O2–C17	–19.7(3)	C1–C6–C7–N1	12.2(5)
N1–Fe1–O2–C17	–73.3(3)	N3–C11–C12–C17	–5.0(6)
O2–Fe1–O1–C1	–175.8(3)	N3–Fe1–O1–C1	93.2(3)
N1–Fe1–O1–C1	35.0(3)	C11–Fe1–N3–C9	83.5(2)
C11–Fe1–N3–C11	–92.2(3)	O2–Fe1–N3–C9	14.6(3)

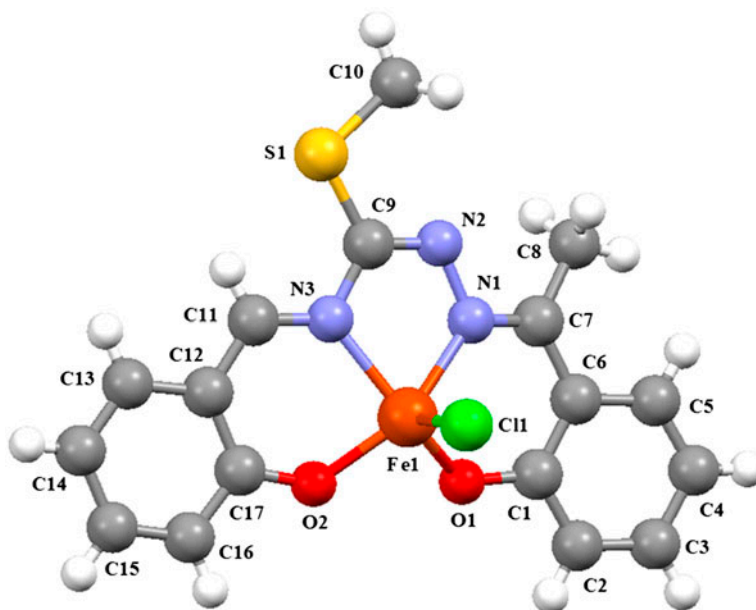
Table 5. Conformational angles (°) for **1** and **1a–b**.

Complex	Fold of ring 1 along O _a ⋯N _a	Fold of ring 2 along N _a ⋯N _b	Fold of ring 3 along O _b ⋯N _b	Angle between mean planes of phenyl rings	Distance of metal from N ₂ O ₂ plane (Å)
1	8.6	11.7	17.9	3.4	0.55
1a	17.8	14.7	18.7	4.0	0.53
1b	19.6	18.3	18.7	7.3	0.61

Notes: (**1**): See figure 3 for key to column headings. M : FeCl, R¹ : Me, R² : Me.

(**1a**): CCDC entry BOZCEY (Ref. [38]), M : FeCl, R¹ : H, R² : Me.

(**1b**): CCDC entry CAWCIM (Ref. [39]), M : OFe(L₄), R¹ : H, R² : Me (su's unavailable for these values).

Figure 2. Molecular structure of **1**. Displacement ellipsoids are drawn at 50% probability level.

singlets in ratio of 2 : 1 because of *cis–trans* isomerism. The singlet signal at 6.67 ppm is assigned to the N⁴H₂ proton resonance. As a result of the template reaction, protons of the phenolic hydroxyl and amine disappear in ¹H NMR spectra of **2** and **3**. These data show that phenolic oxygen loses a proton and a new imine forms by condensation of the free

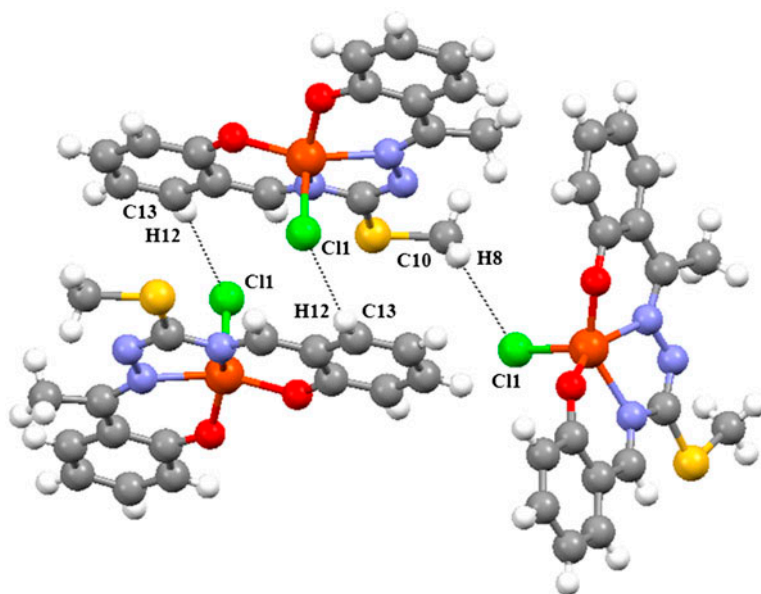


Figure 3. Intermolecular hydrogen bonds of **1**.

NH₂ group with aldehyde. The imine protons of nickel(II) and zinc(II) complexes appear at 8.28 and 8.61 ppm as sharp singlets, respectively [29]. This new ligand system, *N*¹-[(2-hydroxyphenyl)ethylidene]-*N*⁴-[(2-hydroxyphenyl)methylidene]-*S*-methyl-thiosemicarbazidato, coordinates to metal center through the N₂O₂ donor set. The chemical shift of the coordinated ethanol of the zinc(II) complex exhibits an –OH resonance at 4.61 ppm, CH₂ resonance at *ca.* 3.62 ppm and CH₃ resonance at 1.24 ppm. In spectra of nickel(II) and zinc(II) complexes, the aromatic proton signals of aldehyde moiety also confirm the template structure.

3.2.2. FT-IR spectra. In FT-IR spectra of the thiosemicarbazone, the stretching vibration bands of OH, N⁴H₂, C=N¹, and N²=C groups were clearly observed. Template condensation of the thiosemicarbazones can be easily monitored by infrared spectra. The $\nu(\text{OH})$ and $\nu(\text{N}^4\text{H}_2)$ bands are absent in the complex spectra due to coordination of phenolic hydroxyl by losing proton and the formation of a new $\nu(\text{C}=\text{N})$ band between thioamide and salicylaldehyde. The $\nu(\text{C}=\text{N}^1)$ and $\nu(\text{N}^2=\text{C})$ vibrations of ligand are observed at 1600 and 1592 cm⁻¹, respectively. In spectra of **1–3**, C=N vibrations are observed at 1615–1574 cm⁻¹ as three bands of medium intensities, attributed to $\nu(\text{C}=\text{N}^1)$, $\nu(\text{N}^2=\text{C})$ and $\nu(\text{N}^4=\text{C})$. It is difficult to distinguish these imine vibrations. The $\nu(\text{C}=\text{N})$ frequencies of ligand shift to lower energies *ca.* 10–15 cm⁻¹ by chelating and the vibrations of new N⁴=C bonds at *ca.* 1574 cm⁻¹ [30]. The spectrum of the zinc(II) complex displays the $\nu(\text{OH})$ and $\nu(\text{CH})$ vibrations of the coordinated ethyl alcohol at 3445 and 2926–2887 cm⁻¹, respectively [31]. Medium bands from 1428 to 1498 and 1327 cm⁻¹ are assigned to aliphatic CH₃ and CH₂ groups of the ethyl alcohol and *S*-CH₃ group [11, 32].

3.2.3. UV–vis spectra. The electronic spectrum of H_2L^1 shows two absorption bands at 260 and 293 nm (with a shoulder at 302 nm) which can be assigned to $\pi \rightarrow \pi^*$ transitions of aromatic ring. These absorptions are also present in the spectra of **1–3** at 264–265 nm and 278–307 nm, respectively. The $n \rightarrow \pi^*$ transition associated with azomethine and thioamide region of thiosemicarbazone is found at 335 nm [15, 33]. This band in all complexes has a red shift. In the complexes, the $n \rightarrow \pi^*$ transition exhibits blue shift, indicating coordination of azomethine nitrogen. The electronic spectrum of the nickel(II) complex displays a band at 405 nm which is due to $N \rightarrow Ni$ and $O \rightarrow Ni$ (LMCT) charge-transfer transitions [21]. Square planar Ni(II) complexes show three spin-allowed transitions, $^1A_{1g} \rightarrow ^1A_{2g}$, $^1A_{1g} \rightarrow ^1B_{1g}$, and $^1A_{1g} \rightarrow ^1E_g$ [34]. The more intense charge-transfer band obscures the $^1A_{1g} \rightarrow ^1E_g$ transition, and only the $^1A_{1g} \rightarrow ^1A_{2g}$ and $^1A_{1g} \rightarrow ^1B_{1g}$ transitions are observed at 487 and 560 nm, respectively [21, 35]. The zinc(II) complex has two charge-transfer bands at 430 and 473 nm [15, 36]. The moderately intense broad bands for the iron(III) complex at 392 and 462 nm are assigned to LMCT transitions. The spin forbidden d–d transitions bands are not observed in the 500–700 nm region due to the low band intensities.

3.2.4. ESI–MS spectra. Characteristic peaks were observed in the ESI–MS of the starting ligand and metal complexes. The mass spectrum of thiosemicarbazone (H_2L^1) shows peaks at m/z 224.52, 115.11, and 68.48 which correspond to $[M + H]^+$, $[M-C_6H_4OH-CH_3]^+$, and $[M-C_6H_4OH-SCH_3-CH_3]^+$, respectively. The most intense peak in the spectrum of iron(III) complex refers to $[FeLCl-Cl]^+$ ion [37]. The weaker signal at m/z 438.9 can be assigned to $[FeLCl + Na]^+$ ion. The mass spectrum of Ni(II) complex contains two peaks at m/z 384.20 and 406.12, which can be attributed to $[NiL + H]^+$ and $[NiL + Na]^+$, correspondingly. The spectrum of zinc(II) complex displays an intense peak at m/z 390.2 due to the $[ZnL + H]^+$ ion. The peaks at m/z 343.2 and 328.3 are assigned to $[ZnL-SCH_3 + H]^+$ and $[ZnL-SCH_3-CH_3 + H]^+$ ions, respectively, as expected.

3.3. Thermogravimetric analysis

The TGA and derivative thermogravimetric analysis curves for H_2L^1 and **1–3** are represented in figure S1 in the supplemental material. The data obtained from thermogram are given in table 6.

The TG curve of the starting ligand shows an initial 40.3% (Calcd 39.8%) weight loss, which is in agreement with the removal of $NC(S-CH_3)-NH_2$ group at 200–261 °C, followed

Table 6. Thermogravimetric data of the compounds.

Compound	Step	Temp. range (°C)	DTG (°C)	Weight loss (%) found (Calcd)	Residue
H_2L^1	1st	200–261	240	40.30 (39.80)	
	2nd	261–342	289	26.64 (26.80)	
	3rd	342–698	567	33.06 (34.03)	
1	1st	185–350	268	19.49 (19.81)	Fe ₂ O ₃
	2nd	350–525	426	61.36 (63.10)	
2	1st	230–400	336	21.36 (22.96)	NiO
	2nd	400–693	482	59.64 (61.75)	
3	1st	130–232	193	10.55 (10.52)	ZnO
	2nd	232–308	275	13.62 (14.22)	
	3rd	308–653	401	60.77 (60.25)	

by second loss from 261 to 342 °C in which the CH₃CN + OH groups of the ligand are separated with 26.64% (Calcd 26.80%) decrease in weight. The last step (342–698 °C) shows decomposition of phenyl ring with 33.06% (Calcd 34.03%) weight loss.

The thermal decompositions of iron(III) and nickel(II) complexes take place in two steps. In the iron(III) complex, the 19.49% (Calcd 19.81%) weight loss corresponding to losses of *S*-CH₃ + Cl groups occurs at 185–350 °C. The second step with weight loss of 61.36% (Calcd 63.10%) at 350–525 °C is attributed to loss of the remainder of the organic part. The final residue is Fe₂O₃ as indicated by the residual weight of 20.16% (Calcd 21.29%), which is stable above 525 °C. In the first thermal degradation of the nickel(II) complex, NC (*S*-CH₃) + Cl groups are eliminated at 230–400 °C with 21.36% (Calcd 22.96%) weight loss. The rest of the organic moiety is removed in the second step from 400 to 693 °C (59.64% (Calcd 61.75%)).

The TG curve of the zinc(II) complex indicates three steps of decomposition from 130 to 691 °C. The first step at 130–232 °C involves the loss of ethyl alcohol with 10.55% (Calcd 10.52%) weight loss [31]. In the second step, 13.62% loss (Calcd 14.22%) indicates removal of *S*-CH₃ and CH₃ groups at 232–308 °C. The third step is a slow process from 308–691 °C, which is due to the loss of the remainder of ligand, 60.77% (60.25%). The final residue is ZnO with residual weight 19.98% (Calcd 21.50%).

3.4. X-ray study

Black crystals of iron(III) complex (**1**) were grown by slow evaporation of the solution of the complex. Crystal parameters and refinement results of **1** are summarized in table 1. Complex **1** crystallizes in the monoclinic space group *P21/c* with *Z* = 4. The structure of **1** has been solved by direct methods (SIR92) and refined to the residual index *R*₁ = 0.046 for **1**. The relevant bond lengths, bond and torsion angles of **1** are presented in tables 2–4. ORTEP-III drawing with the atom numbering scheme and intermolecular hydrogen bonds of **1** are illustrated in figures 3 and 4.

The angles of the coordination bonds indicate that the O1–N1–N3–O2 donor is at the edges of a deformed square plane and iron is over this square base. Chloride is weakly coordinated to iron, as evidenced by the 2.221(1) Å bond length. The Fe–Cl bond length of **1** agrees well with corresponding distance in similar complexes [20, 28]. The chloride is closer to N1 compared to other edges of the pyramid base, and the square pyramid is distorted in three axes.

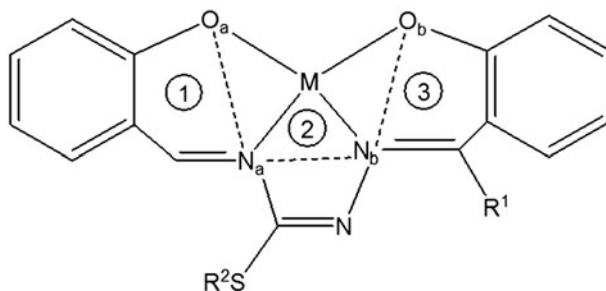


Figure 4. Schematic of **1**, **1a**, and **1b** as a key to table 5.

Table 7. Hydrogen bond parameters in **1** (Å, °).

D–H···A	d(D–H)	d(H···A)	d(D···A)	<(DHA)
C10–H8···Cl1	0.95(6)	2.88(7) ⁱ	3.71(1)	145.28(1)
C13–H12···Cl1	0.95(6)	2.86(7) ⁱⁱ	3.74(1)	159.32(1)

ⁱ+x, +y, +z;ⁱⁱx, 1/2 – y, 1/2 + z.

The condensation of an aldehyde occurs by *syn*-conformation of the *S*-methyl-thiosemicarbazone backbone, and the obtained ONNO-ligand coordinates to the metal ion (figure 2). The iron template shown in figure 2 has a square pyramidal geometry with O1, N1, N3, and O2 of the tetradentate thiosemicarbazone chelating forming a square plane, and chloride in the apical position. The ligand geometry of **1** agrees well with corresponding ligand geometry in a similar complex [38].

The crystal structure of **1** shows intermolecular C–H···O interactions between hydrogens of C10 and C13 of three [Fe(L)Cl] in figure 3. The intermolecular hydrogen bond parameters of **1** are given in table 7.

In coordination of the ligand with iron, three metallo rings are formed: one five-membered FeN₂C₂ and two six-membered FeNC₃O. The Fe1–O1 and Fe1–O2 bonds are relatively short in comparison with Fe1–N1 and Fe1–N3; therefore, five- and six-membered chelate rings are not regular. The principal distortions of the coordination sphere from ideal square pyramidal geometry are the small N1–M–N3 (M = V, Mn, Fe) angle resulting from geometric constraints of the ligand backbone and displacement of the metal from the basal plane toward the axial ligand. The three chelate rings are not coplanar with the metal but each of the rings is folded about a line joining its two donor atoms as depicted by the dashed lines in figure 4. These fold angles in **1** together with the angles between the mean planes of the phenyl rings and the displacement of the metal from the basal plane are presented in table 5 with corresponding data for several related complexes **1a** [38] and **1b** [39]. In the five-coordinate complexes, there is a rough correlation between both the extent of displacement of the metal from the N₂O₂ plane and the folding of the chelate rings and the length of the bond to the axial ligand with the displacement in the order X = O > Cl > Br.

4. Conclusion

We present new unsymmetrical N₂O₂ complexes of iron(III), nickel(II), and zinc(II) synthesized by the template condensation of 2-hydroxy-acetophenone-*S*-methyl thiosemicarbazone with 2-hydroxybenzaldehyde. The compounds have been characterized by analytic, spectral, and TGA. Crystal and molecular structure analyses of [Fe(L)Cl] (**1**) have been carried out by X-ray diffraction. The spectral and X-ray studies show that *N*¹-[(2-hydroxyphenyl)ethylidene]-*N*⁴-[(2-hydroxyphenyl)methylidene]-*S*-methyl-thiosemicarbazone is coordinated to metal ions as a dianionic tetradentate N₂O₂ donor.

Square pyramidal coordination geometry is observed in [Fe(L)Cl] (**1**) and [Zn(L)(C₂H₅OH)] (**2**). The fifth coordination site is occupied by chloride in **1** and oxygen of ethyl alcohol in **3**. [NiL] (**2**) shows the expected square planar, a four-coordinate environment around the nickel center. The thermal decomposition of the complexes by TGA analyses shows that nickel(II) complex is more stable than **1** and **3**. Decomposition temperatures are 185, 230, and 130 °C for **1**, **2**, and **3**, respectively.

Supplementary material

Crystallographic data for the structure in this article have been deposited in the Cambridge Crystallographic Data Center as supplementary publication number CCDC-1005617 for [Fe(L)Cl] (**1**). Copies of the data can be obtained, free of charge, via www.ccdc.cam.ac.uk/conts/retrieving.html or from the Cambridge Crystallographic Data Center, CCDC, 12 Union Road, Cambridge CB2 1EZ, UK [Fax: +44 1223 336033. E-mail: deposit@ccdc.cam.ac.uk].

Acknowledgment

We would like to thank Dr Gulin S. Pozan-Soylu for TGA (thermogravimetric analysis) measurements.

Disclosure statement

No potential conflict of interest was reported by the authors.

Funding

This work was supported by the Research Fund of Istanbul University [grant number/project no. 24533].

Supplemental data

Supplemental data for this article can be accessed here [<http://dx.doi.org/10.1080/00958972.2015.1086760>].

References

- [1] D.X. West, A.E. Liberta, S.B. Padhye, R.C. Chikate, P.B. Sonawane, A.S. Kumbhar, R.G. Yerande. *Coord. Chem. Rev.*, **123**, 49 (1993).
- [2] Y. Yu, E. Gutierrez, Z. Kovacevic, F. Saletta, P. Obeidy, Y.S. Rahmanto, R. Richardson. *Curr. Med. Chem.*, **19**, 2689 (2012).
- [3] H. Beraldo, D. Gambino. *Mini-Rev. Med. Chem.*, **4**, 31 (2004).
- [4] R.J. Glisoni, M.L. Cuestas, V.L. Mathet, J.R. Oubiña, A.G. Moglioni, A. Sosnik. *Eur. J. Pharm. Sci.*, **47**, 596 (2012).
- [5] M. Karatepe, F. Karatas. *Cell Biochem. Funct.*, **24**, 547 (2006).
- [6] S. Halder, S.-M. Peng, G.-H. Lee, T. Chatterjee, A. Mukherjee, S. Dutta, U. Sanyal, S. Bhattacharya. *New J. Chem.*, **32**, 105 (2008).
- [7] J.S. Casas, M.S. García-Tasende, J. Sordo. *Coord. Chem. Rev.*, **209**, 197 (2000).
- [8] T.S. Lobana, R. Sharma, G. Bawa, S. Khanna. *Coord. Chem. Rev.*, **253**, 977 (2009).
- [9] N.V. Gerbeleu, M.A. Yampol'skaya, K.I. Turte, B.Y. Kuyavskaya, S.S. Sokhibov, Kh.M. Yakubov. *Russ. J. Inorg. Chem.*, **32**, 1722 (1987).
- [10] B. Ülküseven, M. Ceritoğlu. *Transition Met. Chem.*, **27**, 390 (2002).
- [11] Y. Kurt, A. Koca, M. Akkurt, B. Ülküseven. *Inorg. Chim. Acta*, **388**, 148 (2012).
- [12] J. Gradinaru, A. Forni, V. Druta, S. Quici, A. Britchi, C. Deleanu, N. Gerbeleu. *Inorg. Chim. Acta*, **338**, 169 (2002).
- [13] V.B. Arion, N.V. Gerbeleu, K.M. Indrichan. *Zh. Neorg. Khim.*, **31**, 126 (1986).
- [14] V.M. Leovac, V.I. Češljević, N. Galešić. *Polyhedron*, **7**, 2641 (1988).

- [15] N.V. Gerbeleu, M.D. Revenko, V.G. Rusu, K.M. Indrichan, M.A. Yampol'skaya. *Russ. J. Inorg. Chem.*, **31**, 691 (1986).
- [16] Y.A. Simonov, S.G. Shova, M.D. Revenko, N.V. Gerbeleu, V.G. Rusu, A.A. Dvorkin. *Izv. Akad. Nauk. Mold. SSR. Ser. Fiz.-Tekh. Mat. Nauk*, **3**, 25 (1988).
- [17] N.V. Gerbeleu, M.D. Revenko, V.G. Rusu. *Russ. J. Inorg. Chem.*, **32**, 529 (1987).
- [18] S. Chandra, X. Sangeetika. *Spectrochim. Acta, Part A*, **60**, 147 (2004).
- [19] Y. Kurt, B. İlhan-Ceylan, M. Açıkgöz, E. Tüzün, G. Atun, B. Ülküseven. *Polyhedron*, **65**, 67 (2013).
- [20] M. Ahmadi, J.T. Mague, A. Akbari, R. Takjoo. *Polyhedron*, **42**, 128 (2012).
- [21] M. Ahmadi, A. Fasihizad, B. Machura, R. Kruszynski, T. Barak. *Polyhedron*, **81**, 115 (2014).
- [22] A. Fasihizad, T. Barak, M. Ahmadi, M. Dusek, M. Pojarova. *J. Coord. Chem.*, **67**, 2160 (2014).
- [23] R. Takjoo, S.W. Ng, E.R.T. Tiekink. *Acta Cryst.*, **E68**, m1033 (2012).
- [24] Ş. Güveli, B. Ülküseven. *Polyhedron*, **30**, 1385 (2011).
- [25] A. Altomare, G. Cascarano, C. Giacovazzo, A. Guagliardi, M. Burla, G. Polidori, M. Camalli. *J. Appl. Cryst.*, **27**, 435 (1994).
- [26] D.J. Watkin, C.K. Prout, J.R. Carruthers, P.W. Betteridge. *Crystals*, Issue 10, Chemical Crystallography Laboratory, Oxford (1996).
- [27] L.J. Farrugia. *J. Appl. Cryst.*, **30**, 565 (1997).
- [28] Y.D. Kurt, B. Ülküseven, S. Tuna, M. Ergüven, S. Solakoğlu. *J. Coord. Chem.*, **62**, 2172 (2009).
- [29] V.B. Arion, P. Rapta, J. Telsler, S.S. Shova, M. Breza, K. Luspai, J. Kozisek. *Inorg. Chem.*, **50**, 2918 (2011).
- [30] V.B. Arion, V.C. Kravtsov, R. Goddard, E. Bill, J.I. Gradinaru, N.V. Gerbeleu, V. Levitschi, H. Vezin, Y.A. Simonov, J. Lipkowski, V.K. Bel'skii. *Inorg. Chim. Acta*, **317**, 33 (2001).
- [31] M. Şahin, T. Bal-Demirci, G. Pozan-Soylu, B. Ülküseven. *Inorg. Chim. Acta*, **362**, 2407 (2009).
- [32] Y.D. Kurt, G.S. Pozan, İ. Kızılcıklı, B. Ülküseven. *Russ. J. Coord. Chem.*, **33**, 844 (2007).
- [33] L.M. Fostiak, I. García, J.K. Swearingen, E. Bermejo, A. Castiñeiras, D.X. West. *Polyhedron*, **22**, 83 (2003).
- [34] A.B.P. Lever. *Inorganic Electronic Spectroscopy*, 2nd Edn, Elsevier, Amsterdam (1984).
- [35] V.T. Kasumov, Ş. Özalp-Yaman, E. Taş. *Spectrochim. Acta, Part A*, **62**, 716 (2005).
- [36] J. Gradinaru, A. Forni, V. Druta, F. Tessore, S. Zecchin, S. Quici, N. Garbalau. *Inorg. Chem.*, **46**, 884 (2007).
- [37] B. Atasever, B. Ülküseven, T. Bal-Demirci, S. Erdem-Kuruca, Z. Solakoğlu. *Invest. New Drugs*, **28**, 421 (2010).
- [38] M.A. Yampol'skaya, S.G. Shova, N.V. Gerbeleu, V.K. Bel'skii, Yu.A. Simonov. *Zh. Neorg. Khim.*, **27**, 2551 (1982).
- [39] M.A. Yampol'skaya, S.G. Shova, N.V. Gerbeleu, Yu.A. Simonov, V.K. Bel'skii, A.A. Dvorkin. *Zh. Neorg. Khim.*, **28**, 1744 (1983).